Polymer 49 (2008) 2770–2774

Contents lists available at ScienceDirect

Polymer

journal homepage: www.elsevier.com/locate/polymer

Phase transition of LCP fluids confined in nanochannels through MD simulation

Kai-Leung Yung [a], Lan He [a,b,*], Yan Xu [a], Jie Kong [a,c]

[a] Department of Industrial and Systems Engineering, The Hong Kong Polytechnic University, Hung Hom, Kowloon, Hong Kong, PR China
[b] College of Mechanical and Electrical Engineering, Northwestern Polytechnical University, Xi'an 710072, PR China
[c] Department of Applied Chemistry, School of Science, Northwestern Polytechnical University, Xi'an 710072, PR China

ARTICLE INFO

Article history:
Received 18 February 2008
Received in revised form 2 April 2008
Accepted 2 April 2008
Available online 12 April 2008

Keywords:
Phase transition
Liquid crystalline polymers
Nanoflow

ABSTRACT

Manipulation of molecular orientation alignment in MCTLCPs (main-chain thermotropic liquid crystalline polymers) by pure shear at nano scale has been investigated for the first time using molecular dynamics (MD) simulation. Results indicate that high planar shear induces long-range uniform orientation ordering (liquid crystalline phase) of initially randomly orientated molecules of MCTLCP fluid confined in a nanochannel, which is confirmed by analyzing the orientation order parameter and the snapshots of MCTLCP liquid in a nanochannel under different shear rates. Insights into the origin of the phase transition phenomena are given at molecular level through investigating the thermodynamic density distribution of MCTLCP molecules in the nanochannel, suggesting that the energy shift due to a radical jump of system density affects both the magnitude and the orientation of the molecular ordering. Simulation results also show that there is a critical shear rate for transforming isotropic phase into liquid crystalline phase. The critical shear rate is dependent on the temperature of the MCTLCP system. Findings in this paper may present useful information for processing TLCP molecules at nano scale and the understanding of nanoflow.

1. Introduction

The structural and dynamic properties of fluids, which are confined in a nanopore or nanochannel, may differ significantly from a macroscopic fluid system due to the geometry of the confinement and the significance of molecular interactions with walls as compared to intermolecular interactions between fluid molecules. Studies on the behavior of fluids in confined micro/nano systems have become intensive recently using experimental, theoretical or computer simulation methods [1–7]. Such systems have some present and many envisioned future applications in the emerging fields of nanoscience and nanotechnology. Therefore, understanding the properties of confined fluids in nano systems, which differ significantly from the bulk fluids, is of fundamental and practical importance.

MCTLCPs have become one of the most promising materials in developing micro/nano components due to the good flowability and high mechanical performance. To some degree, these favorable properties can be attributed to the spontaneous ordering of rigid molecules forming liquid crystalline (LC) phase. Only when LCP liquid stays in the liquid crystalline phase, could its viscosity be remarkably low, resulting in products with excellent dimensional stability and stiffness [8–12]. If LCP liquid is in the isotropic phase, it exhibits mechanical and structural properties similar to conventional flexible polymers. Therefore, controlling the molecular orientation distribution and maintaining the liquid crystalline phase become crucial for micro/nano processing of LCPs.

In a macroscopic system, the liquid crystalline phase can be formed only at certain range of temperature for thermotropic LCP liquids in the absence of external fields. Temperature change can disturb the LC phase and induce phase transition. When there are external fields such as electric or magnetic fields working on low molecular weight liquid crystals, generating and manipulating molecular orientation can be usually achieved through combinations of surface treatments and applied external fields. These methods become impractical when trying to orient high molecular weight LCPs. It is well known that shear flow can be highly effective in inducing macroscopic alignment in materials such as side-chain or main-chain LCPs and block copolymers [13–18]. However, current experimental and theoretical studies still lack a credible complete molecular understanding of these micellar flow-induced orientation alignments; such a model must presumably include inter-atom/molecular reactions, as well as polymeric effects, to account for the structural changes under flow. Hence, it is very necessary to investigate the effect of flow field on kinematics and orientational order of complex polymeric fluids at molecular level

* Corresponding author. Department of Industrial and Systems Engineering, The Hong Kong Polytechnic University, Hung Hom, Kowloon, Hong Kong, PR China. Tel.: +86 852 27667015; fax: +86 852 23625267.
E-mail address: npusujie@126.com (L. He).

0032-3861/$ – see front matter © 2008 Elsevier Ltd. All rights reserved.
doi:10.1016/j.polymer.2008.04.013

by using valid molecular modeling method. It is well known that some hydrodynamic principles in nano systems are different from those of macro systems. However, experimental study of nanoflow is very difficult. Therefore, probing and understanding molecular orientational dynamics of MCTLCP liquids in nanoflow by molecular dynamics simulation become very important.

Previously, the authors had developed a GB–Spring–Bead model for molecular dynamics simulation [19]. Using the model, the phase transition of TLCP due to temperature variation had been described with remarkable accuracy [20]. The effects of wall roughness on the molecular orientation and viscosity of nano polymer flow were also investigated and some interesting phenomena were reported [21].

This paper will investigate the phase transition of confined MCTLCP liquid subject to various planar shears at isotropic temperatures and predict the critical value governing the formation of liquid crystalline phase by MD simulations. Using the GB–Spring–Bead model [19,20] that can describe the mixture of rigidity and flexibility in a real LCP system, MCTLCP molecules will be simulated in constant-NVT and constant-NVE ensembles. Through analyzing the equilibrium configurations of MCTLCP flow at different shear rates and calculating statistically the orientational order parameter, a series of phase evolution will be observed. The origin of the phase transition phenomena will be discussed by analyzing thermodynamic density distribution of LCP molecules in a nanochannel. MD simulations of MCTLCP flow subject to different planar shears will also be conducted at fluctuating system temperatures. Results of this study will reveal the phenomena of phase transition due to shear at isotropic temperature and the existence of critical shear rate for the phase transition and give explanations at molecular level for the first time.

2. Simulation details

The chemical structure of the semiflexible main-chain thermotropic liquid crystalline polymers – poly[(phenylsulfonyl)-*p*-phenylene alkylenebis(4-oxybenzoate)s] (PSHQn) applied in MD simulations, is shown in Eq. (1),

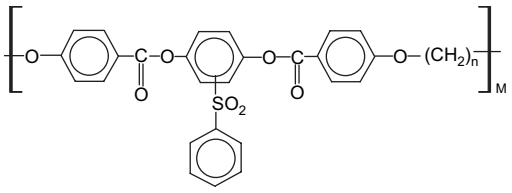

(1)

where n is the number of methylene groups acting as flexible spacers ($n = 3$–12), M is the average degree of polymerization. The LCP molecule is mimicked by our developed GB–Spring–Bead model which has proved efficient and accurate to simulate the high-weight semiflexible LCPs [19,20]. In PSHQn molecules, the mesogenic elements are described by the Gay–Berne (GB) units and the series of methylene groups are represented by two nonlinear springs and a bead, as shown in Fig. 1. Interaction models involved, as seen in Table 1, have been described in detail in the previous literatures [19,20] and values of parameters in potential functions are similar to those used in Refs. [19,20] (as shown in Table 2).

Fig. 1. Schematic diagram of the GB–Spring–Bead model representing two units of one molecular chain in PSHQn.

Table 1
Potentials in GB–Spring–Bead model

Interactions	Potentials	Initial source
Between GB units	Modified GB potential	Ref. [22]
Between beads	Modified (Lennard–Jones) LJ potential	Ref. [19]
Between GB units and beads	Modified generalized potential	Refs. [19,23]
For springs	Nonlinear spring potential	Ref. [19]

The LCP melt is assumed to be subject to planar shear in a nanometer channel by translating the upper wall and the lower wall in opposite directions with varied shear velocity $V_w = c_s\sigma/\tau$ $(\tau = (m\sigma^2/\varepsilon)^{1/2},\ \dot{\gamma} = c_s/\tau)$. The two walls of the shear cell each consists of 2400 atoms distributed between two (111) planes of a fcc (face-centered-cubic) lattice. To eliminate the effect of wall asperities, the walls are assumed to be smooth (with smoothly distributed wall atoms). The configuration of LCP melt flowing in the nanochannel is shown in Fig. 2, where the x-axis is the direction of shear; z-axis is perpendicular to the xy plane. Each atom on the wall is attached to its lattice position by a stiff spring. The potential of spring is expressed by $U_s = 0.5K_wR^2$, where, K_w is the spring stiffness and R is the distance of the atom from its lattice site. The value of the spring stiffness is chosen as $1200\varepsilon/\sigma^2$ so that the ratio of the root-mean-square displacement of the wall atoms and their nearest-neighbor distance was less than the Lindemann criterion for melting [24]. Interactions between liquid molecules and wall atoms are defined by the shifted LJ potential. The energy and the length scales in the LJ potential are supposed to be $\varepsilon_{WG} = 0.6\varepsilon_0^{GB}$, $\sigma_{WG} = 0.75\sigma_0^{GB}$, $\varepsilon_{WL} = 0.6\varepsilon_0^{LJ}$, $\sigma_{WL} = 1.0\sigma_0^{LJ}$, respectively, for interactions between GB units, beads and wall atoms, in order to keep the walls weakly absorbing. The simulation box (xyz), measuring $26.25 \times 3.712 \times 11.7\ \text{nm}^3$, contains 60 LCP molecular chains with the degree of polymerization $M = 12$ and the number of flexible methylene united atoms $n = 10$. Periodic boundary conditions are imposed in $\hat{x}$ and $\hat{y}$ directions.

Polymer molecules are arranged with random centers of mass vectors and velocities of all particles are taken from Maxwell–Boltzmann distributions. Equations of motion are integrated using a leap-frog Verlet algorithm [25]. Initially, calculations are carried out for heating the LCP molecules to an isotropic state. Then, at a constant temperature when the LCP fluid is in isotropic state, ensemble (NVT) simulation of shear flow starts, where the extended system method is used in all the three directions [26]. The time step used in the simulation is 3 fs. Each equilibrium run takes 1×10^6 time steps followed by another 2×10^6 time steps for collecting the results.

During the production run, the orientational order parameter S_2 of the mesogenic units is monitored by Eq. (2) in which S_2 is associated with the largest eigenvalue λ_+ obtained through the diagonalization of the ordering tensor,

Table 2
Values of parameters in interaction potentials

Definition	Values
Length and energy ratio parameters, k, k'	$k = 3$, $k' = 5$
Exponential parameters, μ, ν	$\mu = 2$, $\nu = 1$
Initial well depth parameter for GB units, ε_0^{GB}	$\varepsilon_0^{GB} = 5.61268 \times 10^{-21}$ J
Initial length parameter for GB units, σ_0^{GB}	$\sigma_0^{GB} = 0.4721$ nm
Initial well depth parameter for beads, $\varepsilon_0^{LJ}(\varepsilon)$	$\varepsilon_0^{LJ} = 9.94104 \times 10^{-22}$ J
Initial length parameter for beads, $\sigma_0^{LJ}(\sigma)$	$\sigma_0^{LJ} = 0.3923$ nm
Initial well depth parameter for GB units and beads, $\varepsilon_0^{GB/LJ}$	$\varepsilon_0^{GB/LJ} = 2.3621 \times 10^{-21}$ J
Initial length parameter for GB units and beads, $\sigma_0^{GB/LJ}$	$\sigma_0^{GB/LJ} = 0.4117$ nm
Energy parameters in spring potential, K_s, K_a, K_t	$K_s = 3.6129 \times 10^{-20}$ J $K_a = 8.654 \times 10^{-19}$ J $K_t = 8.654 \times 10^{-19}$ J
The equilibrium angle, α_0	$\alpha_0 = 180^\circ$
The mass of one LJ atom, m	2.34517×10^{-26} kg

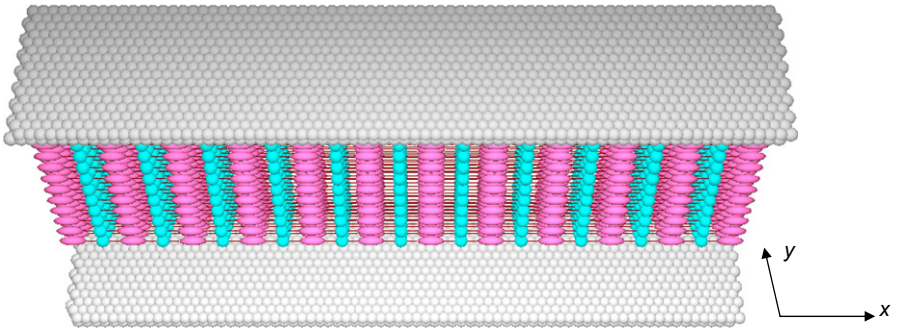

Fig. 2. The initial configuration of LCP molecular chains in the nanochannel.

$$Q_{\alpha\beta} = \frac{1}{N_{GB}}\sum_{i=1}^{N_{GB}}\frac{3}{2}\boldsymbol{u}_{i\alpha}\boldsymbol{u}_{i\beta} - \frac{1}{2}\delta_{\alpha\beta}, \quad \alpha,\beta = x,y,z \tag{2}$$

where, $\boldsymbol{u}_{i\alpha}$ and $\boldsymbol{u}_{i\beta}$ are the components of the orientation unit vectors along molecular long axes of GB particle i. The eigenvector associated with λ_+ provides the director $\boldsymbol{n}$ for describing the average direction of alignment for GB particles.

3. Results and discussions

Firstly, MD simulation is carried out for the melting process of LCP molecules confined in a nanochannel at the system temperature of $T = 454$ K in the absence of planar shear. When the system reaches equilibrium state, the LCP melts show a typical isotropic phase, as shown in Fig. 3. Then it is cooled to $T = 450$ K till it runs to another equilibrium state, where the LCP melts still exhibit isotropic state. Since the formation of liquid crystalline phase normally initiates at temperatures lower than those when TLCP liquid stays in the isotropic phase, it can make sure that the LCP melt should be in the isotropic state at temperatures above $T = 450$ K. The equilibrium configuration at $T = 454$ K is regarded as the initial configuration of the successive run, where the altering shear velocity V_w is uploaded by translating atoms of the upper and lower walls in the opposite direction. The simulation of shear flow begins with a low shear rate ($c_s = 0.1$, $\dot{\gamma} = 4.26 \times 10^{10}\ s^{-1}$), then the shear rate is increased gradually.

3.1. Shear flow-induced phase transition phenomenon

Fig. 4 shows the instantaneous configurations of LCP melts in the nanochannel at different shear rates imposed on wall atoms. As shown in Fig. 4(a), when the shear rate $\dot{\gamma}$ increases gradually from $4.26 \times 10^{10}\ s^{-1}$ to $4.26 \times 10^{11}\ s^{-1}$ ($c_s = 0.1$–1.0) at $T_i = 454$ K, obvious abnormal phenomena do not happen and the flow stays in the isotropic phase as it does in the absence of planar shear (as shown in Fig. 3). When the shear rate $\dot{\gamma}$ increases to $6.39 \times 10^{11}\ s^{-1}$ ($c_s = 1.5$), some entangled LCP molecular chains in the isotropic phase start to disentangle. With the increase of shear rate $\dot{\gamma}$, more units of LCP molecular chains become free from entanglements and tend to align in order, as seen in Fig. 4(b), where the LCP melt exhibits typical biphasic ($\dot{\gamma} = 9.798 \times 10^{11}\ s^{-1}$). As the shear rate $\dot{\gamma}$ goes up to $1.278 \times 10^{12}\ s^{-1}$ ($c_s = 3.0$), LCP molecular chains are elongated sufficiently and show obvious alignment ordering. When the shear rate increases to $1.406 \times 10^{12}\ s^{-1}$ ($c_s = 3.3$), the LCP molecular chains have uniform orientational ordering along the shear direction exhibiting typical liquid crystalline phase and the configuration of the arrangement of molecular chains (as shown in Fig. 4(c)) suggests that the liquid crystalline phase is typically nematic. When decreasing the shear rate to a value below $1.278 \times 10^{12}\ s^{-1}$ ($c_s = 3.0$), the LCP melt still retains in the biphasic state but do not exhibit any clear liquid crystalline phase. Therefore, the shear rate $\dot{\gamma} = 1.278 \times 10^{12}\ s^{-1}$ might be the critical shear rate $\dot{\gamma}_c$ required for the onset of nematic phase formation in the TLCP nanoflow at system temperature of $T_i = 454$ K.

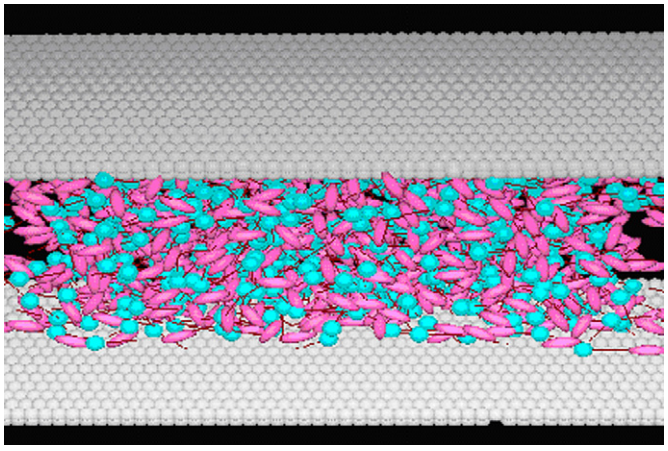

Fig. 3. LCP melt in isotropic phase at $T_i = 454$ K (without planar shear imposed).

The phenomena of flow-induced I–N phase transition can be confirmed further by observing the values of orientation order parameter S_2 at different shear rates. In our studies, the orientation order parameter S_2 is measured by Eq. (2) and the relationship between order parameter and shear rate is shown in Fig. 5. It can be seen that when shear rate increases, the value of orientation order parameter increases as well. At lower shear rate ($\dot{\gamma} < 3.834 \times 10^{11}\ s^{-1}$), the value of orientation order parameter S_2 is less than 0.4. This implies that the LCP molecular chains entangle with each other and there is no apparent alignment, which consists with the snapshot of LCP molecular chains confined in the nanochannel shown in Fig. 4(a). When the shear rate increases from $5.112 \times 10^{11}\ s^{-1}$ to $11.928 \times 10^{11}\ s^{-1}$, the orientation order parameter slowly exceeds 0.5, which suggests that some GB elements in LCP molecular chains start to form alignment. This agrees with the orientation alignment of LCP molecules in the nanochannel shown in Fig 4(b). There is a little jump in the profile of orientation order parameter as the shear rate is greater than $1.278 \times 10^{12}\ s^{-1}$. The larger value of S_2 at higher shear rate suggests that the LCP molecular chains form clearer alignment and the LCP melt is in nematic phase in agreement with what is shown in Fig 4(c). These confirm that $1.278 \times 10^{12}\ s^{-1}$ is the critical shear rate.

3.2. Local density distribution of LCP liquid

The phenomenon of the flow-induced liquid crystalline phase formation can be analyzed by thermodynamic number density

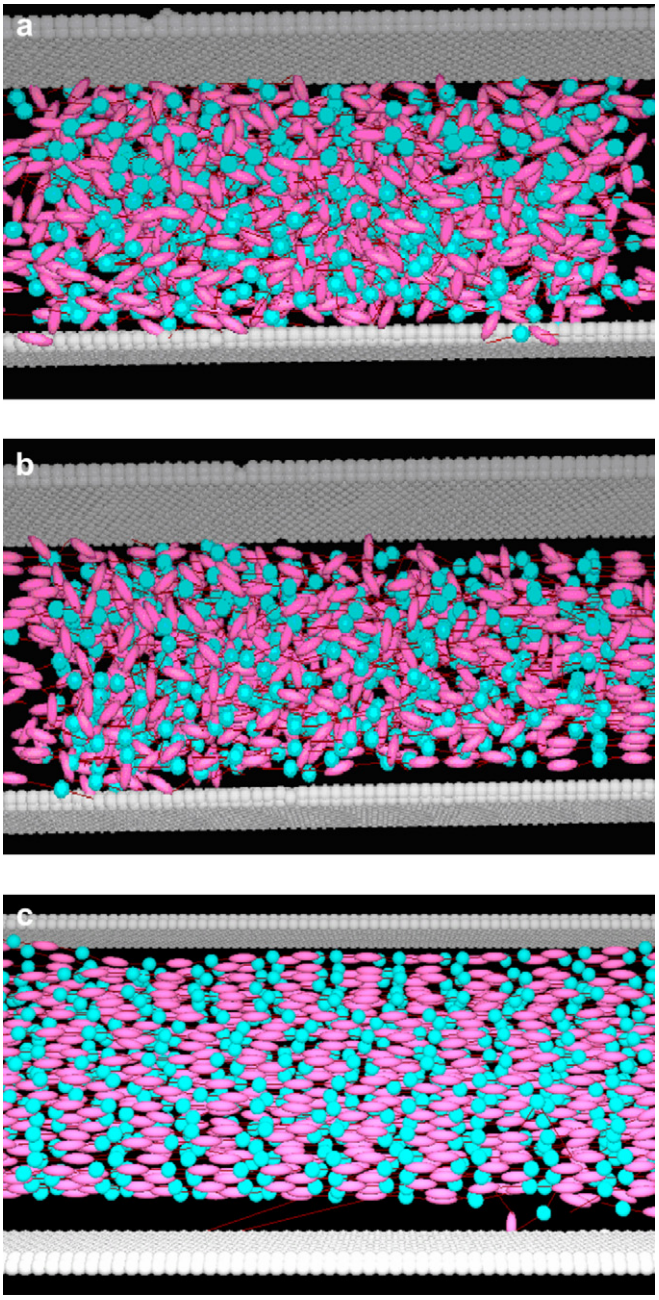

Fig. 4. Snapshots of LCP molecular chains in the nanochannel subject to the varied planar shear at the system temperature $T_i = 454$ K: (a) LCP melt in the isotropic phase ($\dot{\gamma} = 2.556 \times 10^{11}$ s^{-1}); (b) LCP melt in the clear biphasic state ($\dot{\gamma} = 9.798 \times 10^{11}$ s^{-1}) (c) LCP melts in the nematic phase ($\dot{\gamma} = 1.406 \times 10^{12}$ s^{-1}).

profile at different shear rates, which is evaluated by averaging the instantaneous number of particles in the bin widths of 0.25σ (z direction). Fig. 6 presents thermodynamic density profiles at $\dot{\gamma} = 2.556 \times 10^{11}$ s^{-1} (when LCP liquid is in the typical isotropic phase) and $\dot{\gamma} = 1.406 \times 10^{12}$ s^{-1} (when LCP liquid is in the typical liquid crystalline phase) respectively. It is shown that the local density of LCP molecule at $\dot{\gamma} = 2.556 \times 10^{11}$ s^{-1} is not uniform and large fluctuation occurs near the walls. Compared to the density profile at $\dot{\gamma} = 2.556 \times 10^{11}$ s^{-1}, the local density curve at $\dot{\gamma} = 1.406 \times 10^{12}$ s^{-1} seems smoother and more uniform. There are only small variations near the walls. In the middle of the nanochannel, the number density at $\dot{\gamma} = 1.406 \times 10^{12}$ s^{-1} is higher than that at $\dot{\gamma} = 2.556 \times 10^{11}$ s^{-1}. This density jump suggests that shear flow induces actual shift in the thermodynamic

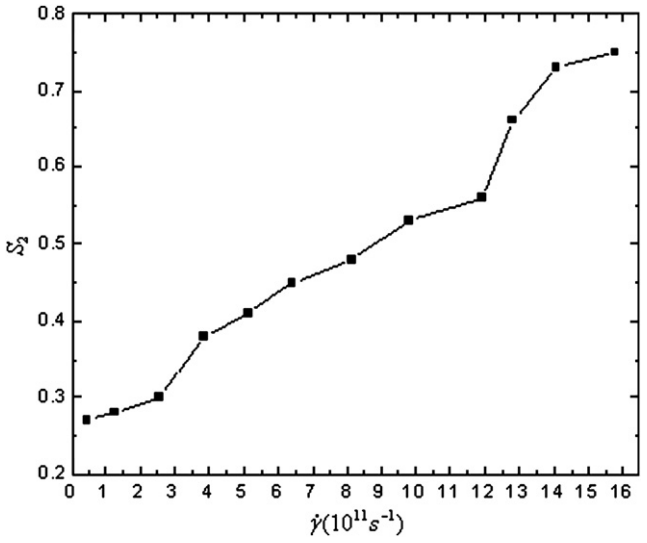

Fig. 5. The orientation order parameter S_2 as the function of the applied shear rate $\dot{\gamma}$ at the system temperature $T_i = 454$ K.

interests like entropy or Helmholtz free energy, which may be validated by density functional theory (DFT) applied for I–N transition in LCPs [27].

The shift effectively affects both the magnitude and the orientation of the molecular ordering. It alters the symmetry-breaking nature of the transition. The phenomena observed in our molecular dynamics simulation verify the prediction of flow-induced phase transition derived by general LE (Leslie–Ericksen) theory [28,29].

3.3. Relationship between the critical shear rate and the system temperature

Besides the critical shear rate $\dot{\gamma}_c$ of 1.278×10^{12} s^{-1} at $T_i = 454$ K, we also measured the critical shear rate $\dot{\gamma}_c$ at different system temperatures by MD simulation. The relationship between critical shear rate $\dot{\gamma}_c$ and temperature T_i is plotted in Fig. 7. It can be seen that $\dot{\gamma}_c$ increases almost linearly with the increase of T_i. This suggests stronger external field force is required to induce I–N phase transition for higher system temperatures to counteract the cohesion between entangled LCP molecular chains.

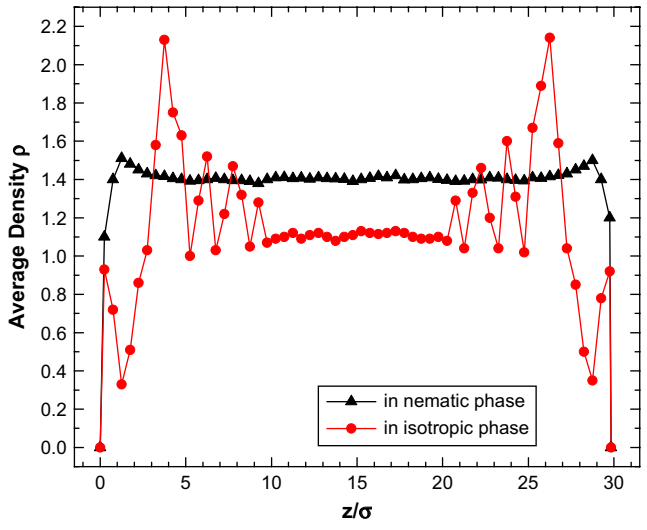

Fig. 6. Thermodynamic density profiles at different shear rates ($T_i = 454$ K) triangles: $\dot{\gamma} = 1.406 \times 10^{12}$ s^{-1}, circles: $\dot{\gamma} = 2.556 \times 10^{11}$ s^{-1}.

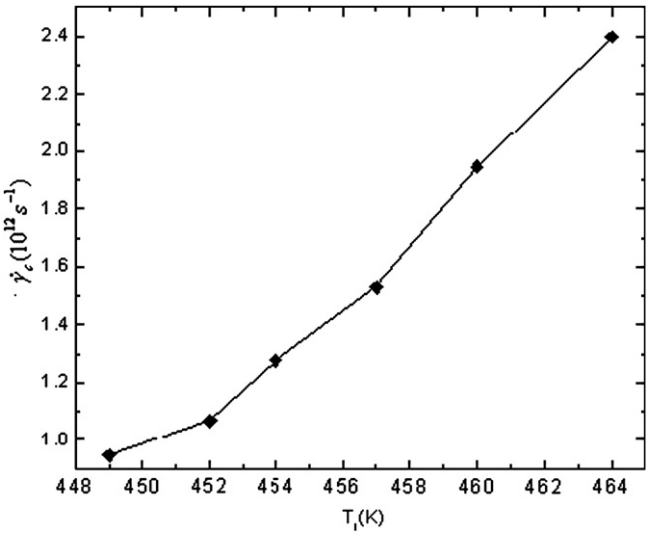

Fig. 7. The critical shear rate $\dot{\gamma}_c$ as the function of temperature T_i for the liquid crystalline phase formation.

4. Conclusions

We have studied the semiflexible main-chain TLCP melt flowing in a nanochannel subject to various planar shears at different system temperatures by MD simulations. By analyzing the orientation order parameter and the snapshots of the LCP melt in the nanochannel at different shear rates, a series of phase transitions from initial isotropic to biphasic then to final nematic phase are observed at the system temperature of $T_i = 454$ K, where TLCP melt normally stays in isotropic phase in the absence of external fields. The phenomenon of the flow-induced liquid crystalline phase transition has been analyzed by thermodynamic number density profile at different shear rates. The density changes at different shear rates suggest that shear flow would induce shift in the thermodynamic interests like entropy or Helmholtz free energy, which affects both the magnitude and the orientation of the molecular ordering. The density jump observed in our study validates the results obtained by density functional theory (DFT) applied for I–N transition in LCPs [27]. In our study, the critical shear rate $\dot{\gamma}_c$ required for the onset of liquid crystalline phase formation in nanochannels is found, and the dependence of critical shear rate on the isotropic temperature is firstly explored at molecular level. Results indicate that the critical shear rate increases linearly with the increase of system temperature. The MD results in our paper verify the predictions of flow-induced phase transition derived by general LE theory [28,29] at molecular level. Findings in this study may provide useful information for processing MCTLCP materials and manipulating molecular orientation of MCTLCPs at nano scale.

Acknowledgment

This work is supported by the Hong Kong Research Grants Council (PolyU5314/05E).

References

[1] Jabbarzadeh A, Atkinson JD, Tanner RI. Phys Rev E 2000;61(1):690.
[2] Priezjev Nikolai V, Troian Sandra M. Phys Rev Lett 2004;92(1):018302.
[3] Yung Kai-Leung, Kong Jie, Xu Yan. Polymer 2007;48:7645.
[4] Brovchenko I, Geiger A, Oleinikova A. J Chem Phys 2004;120:1958.
[5] Megaridis CM, Yazicioglu AG, Libera JA. Phys Fluids 2002;14:15.
[6] Zaini P, Modarress H, Mansoori GA. J Chem Phys 1996;104:3832.
[7] Jeszka Jeremiasz K, Pakula Tadeusz. Polymer 2006;47:7289.
[8] Irwin RS, Sweeny W, Gardner KH, Gochanour CR, Weinberg M. Macromolecules 1986;19:1696.
[9] Sauer Bryan B, Kampert William G, McLean R Scott. Polymer 2003;44:2721.
[10] Romo-Uribe A, Lemmon T, Windle AH. J Rheol 1997;41:1117.
[11] Han CD, Kim SS. J Rheol 1994;38:13.
[12] Rendon Stanley, Burghardt Wesley R, Bubeck Robert A, Lowell Thomas S, Hart Bruce. Polymer 2005;46:10202.
[13] Noirez L. Phys Rev E 2005;72:051701.
[14] Mendil H, Baroni P, Noirez L. Eur Phys J E 2006;19:77.
[15] Chen Zhong-Ren, Kornfield Julia A. Polymer 1998;39:4679.
[16] Han CD, Kim SS. Macromolecules 1995;28:2089.
[17] Mather PT, Romo-Uribe A, Han CD, Kim SS. Macromolecules 1997;30:7977.
[18] Geng Jianxin, Zhao Xiaoguang, Zhou Enle, Li Gao, Lam Wing Yip Jacky, Tang Ben Zhong. Polymer 2003;44:8095.
[19] Yung KL, He Lan, Xu Yan, Shen YW. J Chem Phys 2005;123:246101.
[20] Yung KL, He Lan, Xu Yan, Shen YW. Polymer 2005;46:11881.
[21] Yung KL, He Lan, Xu Yan, Shen YW. Polymer 2006;47:4454.
[22] Gay JG, Bern BJ. J Chem Phys 1981;74:3316.
[23] Cleaver DJ, Care CM, Allen MP, Neal MP. Phys Rev E 1996;54:559.
[24] Barrat L, Hansen JP. Basic concepts for simple and complex liquids. Cambridge: Cambridge University Press; 2003.
[25] Wilson MR, Allen MP, Warren MA, Sauron A, Smith W. J Comput Chem 1997; 18:478.
[26] Iinytskyi JM, Wilson MR. Comput Phys Commun 2002;148:43.
[27] Wessels PPF, Mulder BM. J Phys Condens Matter 2006;18:9335.
[28] Olmsted PD, Goldbart PM. Phys Rev A 1990;41:4578.
[29] Olmsted PD, Goldbart PM. Phys Rev A 1992;46:4966.